2018 IEEE Intelligent Vehicles Symposium (IV)
Changshu, Suzhou, China, June 26-30, 2018

Task Period Selection for Engagement Control of Automatic Clutches*

Xiaoxuan Cheng, Cheng Cheng, Li Chen, *Member, IEEE*

***Abstract*— Task period of the control algorithm in electronically controlled clutches is one of the influencing factors on the engagement quality and computation load. The previous studies provide control algorithms in continuous time-domain, but ignore the performance degradation due to discretization. In order to select an appropriate task period on engagement quality, this paper analyzes the friction-involved clutch engagement dynamics in discrete domain. Models of a closed-loop control system are developed. The models consist of the powertrain with a clutch element, the clutch actuator with time delay, the classical control algorithm combining a feedback and feed-forward link, and a zero-order holder of the task period. After discretization by z-transform, the stability is analyzed, thereafter, the maximum permissible task period, which is 0.3s for the studied system, is determined in terms of stability. Furthermore, the dynamic response is tested in a dSPACE real-time environment. The results show that the maximum vehicle jerk increases rapidly when the task period falls into the unstable region, and the friction loss ceaselessly increases due to the failed synchronization. On the other hand, when the task period falls into the stable area, basically, shorter period gains less vehicle jerk, and the friction loss can be almost the same as that of the continuous system.**

I. INTRODUCTION

Automatic clutches are key enablers to various automatic transmissions in conventional and recently emerging powertrains[1]. The clutch should be carefully controlled during engagement in order to obtain satisfactory quality in terms of vehicle jerk and clutch friction loss. Since the engagement quality is critical for drivability of vehicles and service life of components, various control methods have been studied with the purpose of improvement. For instance, a flatness-based control combining the nonlinear feed-forward and linear feedback loop[2], the ordinary PI control ensuring the tracking accuracy of speed with torque[3] and the nonlinear feedforward-feedback method[4] have been studied. Additionally, optimization control involving multiple algorithms are proposed including the state observer algorithm[5], linear quadratic (LQ) [6]and model predictive control (MPC)[7]. In most of the existing literatures, including the ones mentioned above, the control algorithms are derived in continuous time-domain. However, in real application, the control algorithm is implemented in discrete time-domain because it is translated into code and embedded into a digital control unit. Leveraging on one processor, the electronic control unit always schedules several periodical tasks including the clutch engagement control program. So the control unit has to determine the task period of each task. Due to the friction substantial of the clutch plates, the engagement process consists of three stages, i.e., open, slipping and locked. Among the three, the slipping phase takes the longest time, and the other two involves in discontinuous dynamics. The engagement process may be rather sensitive to the task period because of the complex dynamics.

Basically, shorter period allows closer approximation to the ideal engagement quality pursued by the well-tuned continuous control algorithm, but costs more, and vice versa. Therefore, the maximum permissible task period, which can obtain satisfactory engagement quality but make use of the minimum computation load, is of the interest. As we know, the sampling interval of signals from sensors can be determined according to the Shannon sampling theorem[8]. But the task period is unnecessary to catch up with the sampling interval[9-12]. The reason lies in two: (1) different sensor requires different sampling interval, (2) the signal from a sensor can be stored in a buffer memory and the control algorithm can process the data periodically. The differentiation allows longer task period without breaking the sampling precision. Thus, the computation load can decrease, and the electronic control unit can achieve cost down. The analysis of the task period provides useful reference for more generic applications. Because of the rapid growth of the electronically controlled clutches applied to various transmissions, a systematic method is urgently required to determine the maximum permissible task period which can achieve satisfactory quality during clutch engagement.

This paper aims to select an appropriate task period on the engagement quality with the consideration of computation load and control quality. The dynamic model is developed in discrete time domain. Following that, stability condition is analyzed in order to obtain the upper limitation of the task period. Then, the close-loop control system runs in a digital hardware environment using the dSPACE-based real-time simulators. By varying the task period, the engagement quality is illustrated and analyzed. Finally, the maximum permissible task period can be located in terms of the engagement quality.

II. SYSTEM MODELLING

The diagram of the closed-loop control system is depicted in Figure 1. The system consists of the powertrain, control

*Research supported by the National Natural Science Foundation of China (Grant No. 51475284).

Xiaoxuan Cheng is with Shanghai Jiaotong University, China (e-mail:sky0506@sjtu.edu.cn).

Cheng Cheng is with Shanghai Jiaotong University, China (e-mail: chengcheng19940804@sjtu.edu.cn).

Li Chen is with Shanghai Jiaotong University, China (corresponding author to provide phone: 021-34208149; e-mail: li.h.chen@sjtu.edu.cn).

algorithm, time-delay and zero-order holder. The model of each subsystem is described in the following paragraphs.

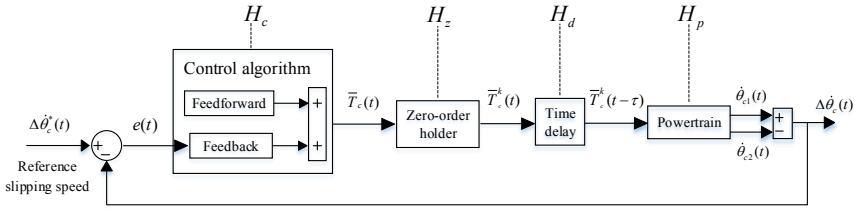

Figure 1. Diagram of close-loop control system during clutch engagement

A. Powertrain Model

The lumped dynamic model of the powertrain is depicted in Figure 2. The model consists of the engine, clutch with separated driving and driven part, vehicle body, elastic connection between the engine and clutch, elastic connection between the clutch and vehicle body.

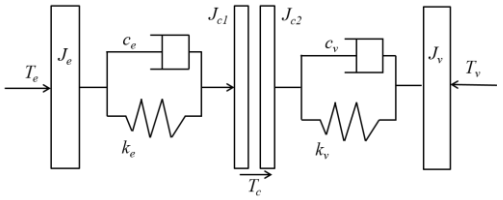

Figure 2. Powertrain model

The model has four degree-of-freedom of motion. The governing equations are written as below. Equation (1) and (2) represent the dynamics of the engine-side components separated by the clutch. Similarly, (3) and (4) represent the dynamics of the body-side components.

$$J_e\ddot{\theta}_e = T_e - c_e(\dot{\theta}_e - \dot{\theta}_{c1}) - k_e(\theta_e - \theta_{c1}) \quad (1)$$

$$J_{c1}\ddot{\theta}_{c1} = c_e(\dot{\theta}_e - \dot{\theta}_{c1}) + k_e(\theta_e - \theta_{c1}) - T_c \quad (2)$$

$$J_{c2}\ddot{\theta}_{c2} = T_c - c_v(\dot{\theta}_{c2} - \dot{\theta}_v) - k_v(\theta_{c2} - \theta_v) \quad (3)$$

$$J_v\ddot{\theta}_{c2} = c_v(\dot{\theta}_{c2} - \dot{\theta}_v) + k_v(\theta_{c2} - \theta_v) - T_v \quad (4)$$

where J_e denotes the inertia moment of the engine, J_{c1} denotes the inertia moment of the driving part of the clutch in the engine side, J_{c2} denotes the inertia moment of the driven part of the clutch in the body side, J_v is the equivalent inertia moment of the components from the transmission shaft to vehicle body, k_e and k_v denote the stiffness, c_e and c_v denote the damping coefficient, T_e denotes the output torque of the engine, T_c denotes the transmitted torque of the clutch, T_v denotes the vehicle load torque, θ_e, θ_{c1}, θ_{c2} and θ_v denote the angular displacement of the engine, engine-side part of the clutch, body-side of the clutch and output shaft to the vehicle body, respectively.

The clutch torque can be described with respect to the status of the clutch as below:

$$T_c = \begin{cases} 0 & \text{open} \\ \mu \cdot F_n \cdot R_c \cdot N \cdot \text{sign}(\Delta\dot{\theta}_c) & \text{slipping} \\ [-\mu_s \cdot F_n \cdot R_c \cdot N \quad \mu_s \cdot F_n \cdot R_c \cdot N] & \text{locked} \end{cases} \quad (5)$$

in which, μ and μ_s denote the kinetic and static friction coefficient of the clutch friction plate, respectively; F_n is the normal force on the friction plate; R_c is the equivalent acting radius of the normal force; N is the number of the friction interfaces of the clutch, $\Delta\dot{\theta}_c$ is the slipping speed on the friction interface of the clutch. The definition of $\Delta\dot{\theta}_c$ is given by:

$$\Delta\dot{\theta}_c = \dot{\theta}_{c1} - \dot{\theta}_{c2} \quad (6)$$

It can be seen from (5) that the clutch transmitted torque T_c is controllable only in the slipping stage by applying a proper normal force F_n, while the other two stages cannot be controlled by the normal force F_n. The clutch torque T_c is zero in the open stage, and can be any value within the range defined by the normal force F_n in the locked stage. Upon this understanding, the normal force F_n is critical for the clutch engagement quality because it has to connect the three stages (open, slipping and locked) smoothly.

In the slipping stage, the magnitude of the clutch torque T_c is determined by the product term $(\mu \cdot F_n \cdot R_c \cdot N)$, and the sign of T_c is determined by the function $\text{sign}(\Delta\dot{\theta}_c)$. That means, the magnitude of T_c is proportional to the magnitude of the normal force F_n, and the direction of T_c is determined dynamically by the slipping speed $\Delta\dot{\theta}_c$. For the simplicity of the following derivation, let the magnitude of the clutch torque in the slipping stage be represented by $\overline{T_c}$, i.e., $\overline{T_c} = \mu \cdot F_n \cdot R_c \cdot N$, the expression of the slipping stage in (5) can be rewritten as:

$$T_c = \overline{T_c} \cdot \text{sign}\left(\Delta\dot{\theta}_c\right) \quad \text{slipping} \quad (7)$$

Referring to the literatures on powertrain dynamics and control, the calculation of the vehicle load T_v can be calculated as below[13]:

$$T_v = (F_{air} + F_g + F_r) \cdot R \quad (8)$$

in which, R is the tire radius, F_{air}, F_g, F_r is the wind resistance, ramp resistance and rolling friction resistance respectively. They are calculated as below:

$$F_{air} = 0.5 \cdot c_D \cdot A_V \cdot \rho_{air} \cdot (v_{air} + v)^2 \quad (9)$$

$$F_g = m \cdot g \cdot \sin\alpha \quad (10)$$

$$F_r = m \cdot g \cdot \cos\alpha \cdot f \quad (11)$$

where, c_D is the wind resistance coefficient, A_V is the car upwind area, ρ_{air} is the air density, v_{air} is the head wind speed, v is the vehicle speed, m is the vehicle mass, g is the gravity, α is the road slope, f is the rolling resistance friction coefficient. The vehicle speed v and the angular velocity $\dot{\theta}_v$ of the output shaft are subject to a kinematic constraint as below:

$$v = i_g \cdot \dot{\theta}_v \tag{12}$$

in which, i_g denotes the speed ratio.

B. Control Algorithm

The control algorithm during clutch engagement has been studied for years[2-7]. In order to emphasize the effect of the task period, this paper adopts a classical control algorithm which can achieve satisfactory engagement quality.

The magnitude of the clutch transmitted torque $\overline{T}_c(t)$ is defined as the control input as shown in Figure 1. The control algorithm consists of a feedforward block and a feedback loop. The engine output torque T_e is taken as the feed-forward part of the control input. The feedback loop applies a proportional gain K_p with respect to deviation from the reference slipping speed of the clutch. The control algorithm can be expressed as:

$$\overline{T}_c(t) = T_e(t) + K_p e(t) \tag{13}$$

in which, $e(t) = \Delta\dot{\theta}_c(t) - \Delta\dot{\theta}_c^*(t)$,and $\Delta\dot{\theta}_c^*$ is the reference slipping speed of the clutch.

It can be seen that the feed-forward block has nothing to do with the either the reference input $\Delta\dot{\theta}_c^*$ or the output $\Delta\dot{\theta}_c$. So the feed-forward block can be regarded as a predefined disturbance, which does not affect the system stability but affects the dynamic response. Therefore, only the transfer function $H_c(s)$ of the feedback block is derived by applying Laplace transform to (13) as below:

$$H_c(s) = K_p \tag{14}$$

C. Time Delay

The time delay subsystem is used to describe the inevitable delay of the actuators due to various factors, such as the mechanical inertia, electromotive of the motor-driven system, the filling phase of the hydraulic system, and etc.

Let τ denote the delay time, then the transfer function $H_d(s)$, whose output is $\overline{T}_c^k(t)$ and output is $\overline{T}_c^k(t-\tau)$, is derived by applying Laplace transform as below:

$$H_d(s) = e^{-\tau s} \tag{15}$$

D. Zero-order Holder

The zero-order holder is used to model the holding of the signal sampled and calculated at the task period. Let T denote the task period and $kT\,(k = 0,1,\cdots,n)$ the discrete calculation time. The zero-order holder is to maintain the value of $\overline{T}_c(t)$ between the time kT and $(k+1)T$. The mathematical expression is given as below:

$$\overline{T}_c^k(t) = \overline{T}_c(kT) \quad (k = 0,1,\cdots,n) \tag{16}$$

where $kT \le t \le (k+1)T$.

The transfer function $H_z(s)$ of the zero-order holder is derived by applying Laplace transform to (17) as below:

$$H_z(s) = \frac{1 - e^{-sT}}{s} \tag{17}$$

III. STABILITY ANALYSIS

As observed from (1) to (4), the two equations of the engine-side dynamics are similar to those two of the body-side dynamics. Each of the two parts describes a two degree of freedom motion subject to stiffness and damping element, and uses four order ordinary differential equations. Moreover, the state variables of the two parts are independent on each other. Therefore, the stability analysis of the two parts is similar and can be conducted respectively. The following paragraphs provide the derivation of the body-side dynamics. The method can be used for the engine-side dynamics, though, with different parameter values.

At first, the transfer function in continuous-time domain described in Laplace transform is derived for each subsystem in Figure 1. Secondly, discretization is implemented by applying z -transform to the Laplace transform. Thirdly, the stability is analyzed by calculating the characteristic roots of the transfer function in z -domain. Further, using the method of root locus, the influences of key parameters on the stability can be illustrated.

A. Discretization by z-transform

Because the clutch torque $T_c(t)$ is piece-wise nonlinear as per the expression in (5), it can be linearized for $\mathrm{sign}(\Delta\dot{\theta}_c) = 1$ under the assumption of $\Delta\dot{\theta}_c > 0$. Thereafter, the transfer function $H_p(s)$, whose input is the clutch transmitted torque $\overline{T}_c(t)$ and output is the angular velocity $\dot{\theta}_c$ of the output shaft, can be derived from (3) and (4) as below:

$$H_p(s) = \frac{(J_v s^2 + c_v s + k_v)}{J_{c2} J_v s^3 + (J_{c2} c_v + J_v c_v) s^2 + (J_{c2} k + J_v k_v) s} \tag{18}$$

The transfer functions of the other three subsystems, i.e., the control algorithm, time-delay and the zero-order holder, have been obtained in (14), (15) and (17), respectively. Therefore, the open loop transfer function $H(s)$ can be written as below:

$$H(s) = H_c(s) \cdot H_z(s) \cdot H_d(s) \cdot H_p(s) \tag{19}$$

Thereafter, the z -transform of $H(s)$ can be written as:

$$\begin{aligned} H(z) &= Z[H(s)] \\ &= k_p z^{-\frac{\tau}{T}} \cdot (1 - z^{-1}) \cdot Z\left[\frac{J_v s^2 + c_v s + k_v}{J_{c2} J_v s^4 + (J_{c2} + J_v) c_v s^3 + (J_{c2} + J_v) k_v s^2}\right] \end{aligned} \tag{20}$$

The corresponding closed-loop transfer function in z -transform can be written as:

$$G(z) = \frac{H(z)}{1 + H(z)} \tag{21}$$

So, the characteristic equation of the closed-loop control system is:

$$1 + H(z) = 0 \tag{22}$$

In the expressions (19) to (22), the task period T is to be determined. Once it is determined, the transfer functions (21) and (22) can be written in an explicit format, and the numerical solution of the characteristic roots in (22) can be obtained.

B. Characteristic Roots

At first, the characteristic roots at the task period $T = 0.2s$ and $T = 0.4s$ are resolved, respectively. The stability is determined by the location of the characteristic roots. Then, the root locus is given in terms of the task period T. The parameters used in the analysis are listed in Table 1.

Let $T = 0.2s$, the open-loop transfer function $H(z)$ is derived as:

$$H(z) = \frac{0.01322z^2 + 0.0008152z - 7.987\times10^{-5}}{z^3 - 0.9558z^2 - 0.04172z - 0.002479} \quad (23)$$

The characteristic root of the closed-loop transfer function is calculated as:

$$z_1 = 0.110\ ,\ z_2 = -0.245 - 0.187i\ ,\ z_3 = -0.245 + 0.187i \quad (24)$$

Obviously, the modules of the above three roots are all less than 1, i.e., they are all located inside the unit circle in the z –plane, therefore, the closed-loop system is stable.

On the other hand, let $T = 0.4s$, the open-loop transfer function $H(z)$ is derived as:

$$H(z) = \frac{0.02667z^2 + 7.012\times10^{-5}z + 5.155\times10^{-6}}{z^3 - 0.997z^2 - 0.002998z - 6.144\times10^{-6}} \quad (25)$$

The characteristic root of the closed-loop transfer function is calculated as:

$$z_1 = -1.69\ ,\ z_2 = -0.001 - 0.017i\ ,\ z_3 = -0.001 + 0.017i \quad (26)$$

It can be seen that the first root z_1 is located outside the unit circle in the z –plane, therefore, the closed-loop system is unstable.

TABLE I. PARAMETERS USED IN ANALYSIS

Symbol	Value	Symbol	Value
m	16000 kg	k_e	1000 Nm/rad
J_e	2 kg·m^2	c_e	10 kg·m^2
J_c	5 kg·m^2	k_v	10000 Nm/rad
J_v	30 kg·m^2	c_v	100 kg·m^2
μ_s	0.44	μ	0.40
N	2	R_c	0.15 m
c_D	0.32	f	0.0015
A_V	1.8 m^2	ρ_{air}	1.205 kg/m^3
i_g	3.5	R	0.525 m
τ	20 ms		

More calculations for $0.001s \le T \le 0.5s$ are implemented every $0.001s$, which can be plotted as shown in Figure 3. The horizontal axis is the task period T, and the vertical axis is the maximum module of the three characteristic roots. It can be seen that the maximum module is less than 1 when $T < 0.3s$, while larger than 1 when $T > 0.3s$. Therefore, the closed-loop system can be stable when the task period is $T < 0.3s$. In other words, the maximum permissible task period, represented by $T_{\max}$, is $0.3s$.

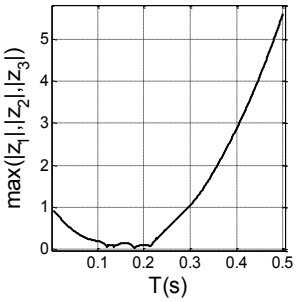

Figure 3. Maximun module of the characteristic roots with respect to task period T

C. Influencing Factors

It is of interest that some system parameters may change the maximum permissible task period $T_{\max}$. Four key parameters are selected as the influencing factors, i.e., the natural frequency w_n, the damping coefficient ξ_n, the delay time τ and control gain k_p. The natural frequency w_n and the damping coefficient ξ_n are defined as $w_n = \sqrt{k_v / J_v}$ and $\xi_n = c_v / \sqrt{k_v J_v}$, respectively. In Figure 3, the values of ω_n, ξ_n and τ are $w_n = 20rad/s$, $\xi_n = 0.32$ $\tau = 20ms$ and $k_p = 5$. Taking the other three parameters unchanged, the root locus with respect to w_n, ξ_n, τ and k_p is plotted in Figure 4 - Figure 7, respectively.

It can be seen that the maximum permissible task period $T_{\max}$ decreases along with the increasing w_n, decreasing ξ_n, increasing τ or increasing k_p. Moreover, the maximum permissible task period $T_{\max}$ restricted by the delay τ and ξ_n is much less than those from w_n and k_p.

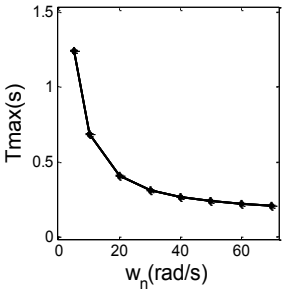

Figure 4. Maximum permissible task period with respect to the natural frequency w_n

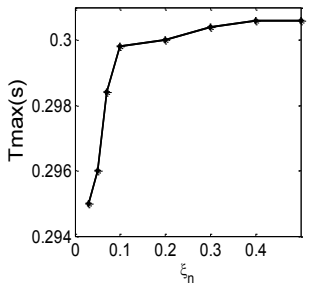

Figure 5. Maximum permissible task period with respect to the damping coefficient ξ_n

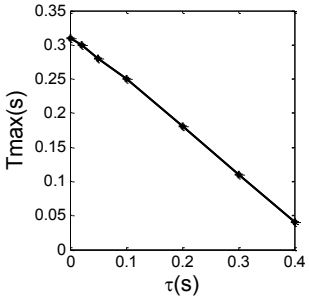

Figure 6. Maximum task period

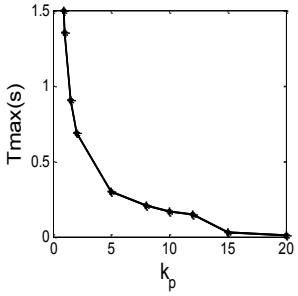

Figure 7. Maximum task period with

with respect to the time delay τ respect to the control gain k_p

IV. Dynamic Response In Dspace Real-time Test Environment

The clutch engagement quality is evaluated by the vehicle jerk and clutch friction loss. Although the stability analysis in the previous section is useful, it does not provide detailed information on the dynamical behavior and engagement quality of the system. As a matter of fact, the stability condition is an extreme boundary which limits the maximum task period of the system. This boundary does not necessarily mean that the engagement quality is good when the period is within the stable region. This section implements tests in a dSPACE real-time environment in order to expose the influence of the task period on the clutch engagement quality.

The dSPACE environment consists of two MicroAutoboxes as shown in Figure 7. One MicroAutobox is used to run the control algorithm and implement the task period; the other one is used to run the powertrain model and simulate the time delay. The two MicroAutoboxes communicate through a timer-triggered I/O connection.

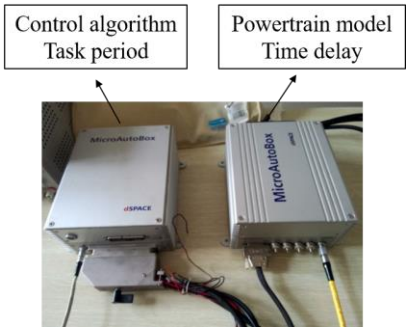

Figure 8. DSPACE real-time test environment

The dynamic responses during the clutch engagement under different task periods are illustrated in Figure 8, with the engine torque set as a constant $T_e = 100Nm$. When the task period increases to be $T = 0.1s$, the driving and driven part of the clutch can synchronize after slipping for a period of time as shown in Figure 8(a). However, the vehicle jerk increases to as much as 50m/s^3, which exceed the acceptable limitation of 10 m/s^3[14]. It should notice that the task period $T = 0.1s$ falls into the stable region as per the stability analysis by root locus illustrated in Figure 3.

When the task period increases to be $T = 0.3s$ which is just entering into the unstable region, the dynamic response is given in Figure 8(b). Due to the task period, the control input T_c is obviously observed with a zero-order holder. The clutch synchronization cannot be completed due to the intensive vibration. The vehicle jerk increases up to several hundreds which will do harm to the driveline components and destroy the riding comfort.

When the task period increases to be $T = 0.35s$ which falls into the unstable region. The results are much worse according to Figure 8(c). The control input T_c increases rapidly, and the vehicle jerk is up to several thousands. The driving and driven part of the clutch cannot synchronize due to the divergent vibration.

Regarding the friction loss during clutch engagement, the system using the task period $T = 0.1s$ generates almost the same loss as the continuous system. However, the system using the task period $T = 0.3s$ increases the friction loss ceaselessly due to the failed synchronization. Under the extreme case using the task period $T = 0.35s$, the friction loss is three times as that of the continuous system during the 10s running time.

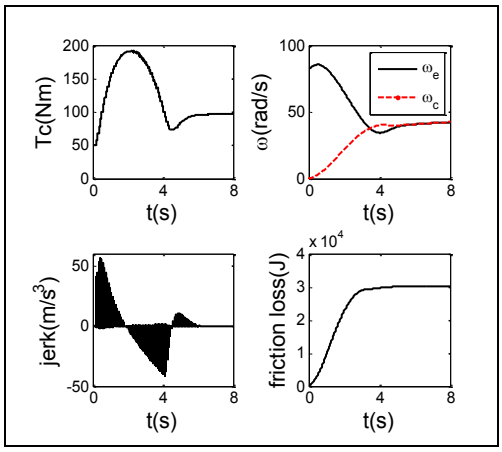

(a) $T = 0.1s$

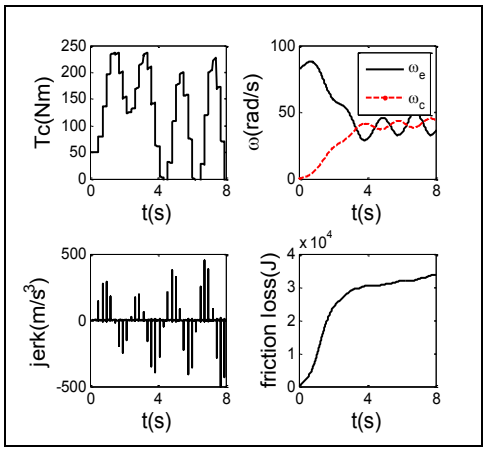

(b) $T = 0.3s$

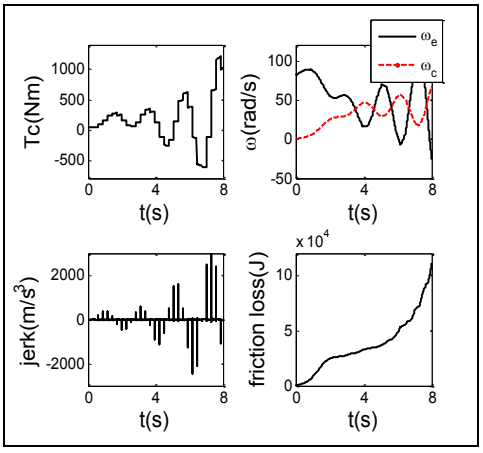

(c) $T = 0.35s$

Figure 9. Dynamic responses under different task period

The tests for the task period from 0.001s to 0.4s are implemented every 0.001s. The test runs for 10s for each case. The vehicle jerk is calculated and the maximum value is recorded. The maximum vehicle jerk with respect to the corresponding task period is plotted in Figure 9. It can be seen that the maximum vehicle jerk increases rapidly when the task period T is greater than 0.3s, which is the critical point separating the stable and unstable region. For those less than 0.3s, small task period results in small jerk. Especially, the maximum vehicle jerk can be less than 10m/s^3 when the task period $T < 0.02s$.

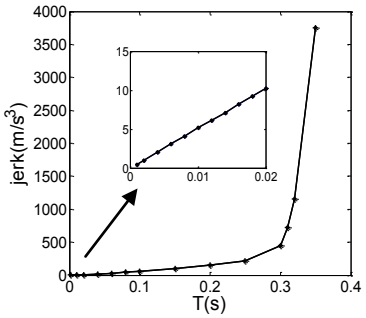

Figure 10. Maximum vehicle jerk with respect to different task period

V. CONCLUSION

In order to locate the maximum permissible task period, this paper analyzes the friction-involved clutch engagement dynamics in discrete domain. At first, models of a closed-loop control system are developed. The models consist of the powertrain with a clutch element, the clutch actuator with time delay, the classical control algorithm combining a feedback and feed-forward link, and a zero-order holder of the task period.

The closed-loop control system is discretized by z-transform. The stability is analyzed in z-domain. The upper limitation of the task period is 0.3s for the system with the listed parameters. The root locus illustrates that low natural frequency, low damping coefficient and short time delay can tolerate large task period.

The dynamic response is tested in a dSPACE real-time environment. The results show that the maximum vehicle jerk increases rapidly when the task period falls into the unstable region, and the friction loss ceaselessly increases due to the failed synchronization. On the other hand, when the task period falls into the stable area, basically, shorter period gains less vehicle jerk, and the friction loss can be almost the same as that of the continuous system. Specifically, the maximum vehicle jerk can be less than 10m/s^3 when the task period is less than $0.02s$ for the system with the listed parameters.

The methodology developed in this paper provides useful reference to determine the maximum permissible task period in terms of stability and dynamic response, respectively.

ACKNOWLEDGMENT

This project is supported by the National Natural Science Foundation of China (Grant No. 51475284).

REFERENCES

[1] S. Bai, J. M. Maguire, and H. Peng, "Dynamic Analysis and Control System Design of Automatic Transmissions," *SAE Technical Paper,* 2013.

[2] J. Horn, J. Bamberger, P. Michau, and S. Pindl, "Flatness-based clutch control for automated manual transmissions," *Control Engineering Practice,* vol. 11, pp. 1353-1359, 2003/12/01/ 2003.

[3] L. Glielmo, L. Iannelli, V. Vacca, and F. Vasca, "Gearshift control for automated manual transmissions," *Control Engineering Practice,* vol. 11, pp. 17-26, 2006.

[4] B. Gao, H. Chen, Q. Liu, and K. Sanada, "Clutch slip control of automatic transmissions: A nonlinear feedforward-feedback design," in *2010 IEEE International Conference on Control Applications*, 2010, pp. 884-889.

[5] P. Dolcini, H. Bechart, and C. C. d. Wit, "Observer-based optimal control of dry clutch engagement," in *Proceedings of the 44th IEEE Conference on Decision and Control*, 2005, pp. 440-445.

[6] L. Glielmo and F. Vasca, "Optimal Control of Dry Clutch Engagement," *SAE Technical Paper,* 2000.

[7] R. Amari, P. Tona, and M. Alamir, "Experimental evaluation of a hybrid MPC strategy for vehicle start-up with an Automated Manual Transmission," in *2009 European Control Conference (ECC)*, 2009, pp. 4271-4277.

[8] A. J. Jerri, "The Shannon sampling theorem-Its various extensions and applications: A tutorial review," *Proceedings of the IEEE,* vol. 65, pp. 1565-1596, 1977.

[9] L. E. d. L. d. Oliveira, L. E. B. d. Silva, V. F. d. Silva, G. L. Torres, and E. L. Bonaldi, "Real-time determination of the best interval of calculation for moving averages used for DC value extraction in active power filter control methods," in *IEEE 2002 28th Annual Conference of the Industrial Electronics Society. IECON 02*, 2002, pp. 1526-1531 vol.2.

[10] M. Montanari, F. Ronchi, C. Rossi, A. Tilli, and A. Tonielli, "Control and performance evaluation of a clutch servo system with hydraulic actuation," *Control Engineering Practice,* vol. 12, pp. 1369-1379, 2004/11/01/ 2004.

[11] Y. A. W. Shardt and B. Huang, "Closed-loop identification with routine operating data: Effect of time delay and sampling time," *Journal of Process Control,* vol. 21, pp. 997-1010, 2011/08/01/ 2011.

[12] S. Gao and D. Huang, "Analysis of Influence of Sampling Interval and VTEC Model on Estimation of GPS Instrumental Biases," *Journal of Geodesy & Geodynamics,* vol. 30, pp. 112-115, 2010.

[13] L. Chen, G. Xi, and J. Sun, "Torque Coordination Control During Mode Transition for a Series-Parallel Hybrid Electric Vehicle," *IEEE Transactions on Vehicular Technology,* vol. 61, pp. 2936-2949, 2012.

[14] Y.-S. Zhao, L.-P. Chen, Y.-Q. Zhang, and J. Yang, "Enhanced Fuzzy Sliding Mode Controller for Automated Clutch of AMT Vehicle," *SAE Technical Paper*, 2006.